applied sciences

MDPI

Article

Bluesil FLD 550 HT Silicone Oil as Heat Transfer Fluid for Power Plant Applications: Thermal Stability Properties

Emiliana Mansi [1,*], Irena Balog [2], Giampaolo Caputo [3], Natale Corsaro [2], Ilaria Di Sarcina [4], Giuliano Tiranti [4], Francesco Filippi [5], Fabio Panza [1], Nicolò Ratto [6], Salvatore Sau [2], Andrea Simonetti [4], Annarita Spadoni [2], Anna Chiara Tizzoni [2], Alessia Cemmi [4] and Marco Ciotti [1]

1 ENEA Nuclear Department, NUC-PLAS Division, Via Enrico Fermi 45, 00044 Frascati, Italy
2 ENEA Energy Technologies and Renewable Sources Department, TERIN-SSI-EAT Laboratory, Via Anguillarese 301, 00123 Rome, Italy; irena.balog@enea.it (I.B.); natale.corsaro@enea.it (N.C.); salvatore.sau@enea.it (S.S.); annachiara.tizzoni@enea.it (A.C.T.)
3 ENEA Energy Technologies and Renewable Sources Department, TERIN-SSI-EDS Laboratory, Via Anguillarese 301, 00123 Rome, Italy
4 ENEA Nuclear Department, NUC-IRAD-GAM Laboratory, Via Anguillarese 301, 00123 Rome, Italy
5 ENEA Nuclear Department, NUC-PLAS-FIPI Laboratory, Via Enrico Fermi 45, 00044 Frascati, Italy
6 ENEA Nuclear Department, NUC-IRAD-CRGR Laboratory, Via Anguillarese 301, 00123 Rome, Italy
* Correspondence: emiliana.mansi@enea.it

Abstract: Thermal oils have been utilized as heat transfer fluids for several decades in many applications, including industrial facilities, power plants and solar receiver systems. Despite their large employment, very few data are available about oils behavior under thermal stress and related degradation processes. For these reasons, the thermal stability of a silicone-based diathermic oil, Bluesil FLD 550 HT, was investigated in the present work. A laboratory-scale set-up was assessed to perform controlled heating tests, and fresh and thermally aged oils samples were analyzed to determine changes in chemical composition and thermo-physical features. Degradation products in the gaseous and vapor phase were also detected and analyzed by online and offline measurements. The obtained results are compared with the ones present for aromatic oils, largely employed as heat transfer media. Bluesil showed a higher thermal resistance compared to aromatic materials, and, thanks to its low volatility together with a high chemical stability, it was successfully tested up to 500 °C. According to its polymeric structure, thermal degradation processes occur mainly through Si-O bond scission, leading to both the segmentation of silicone chains and the formation of cross-linked species as byproducts.

Keywords: silicone oil; heat transfer fluids; thermal oil; cooling fluids; thermal stability; chemical characterization

check for updates

Academic Editor: Andrea Frazzica

Received: 29 January 2025
Revised: 14 February 2025
Accepted: 19 February 2025
Published: 21 February 2025

Citation: Mansi, E.; Balog, I.; Caputo, G.; Corsaro, N.; Di Sarcina, I.; Tiranti, G.; Filippi, F.; Panza, F.; Ratto, N.; Sau, S.; et al. Bluesil FLD 550 HT Silicone Oil as Heat Transfer Fluid for Power Plant Applications: Thermal Stability Properties. *Appl. Sci.* **2025**, *15*, 2340. https://doi.org/10.3390/app15052340

Copyright: © 2025 by the authors. Licensee MDPI, Basel, Switzerland. This article is an open access article distributed under the terms and conditions of the Creative Commons Attribution (CC BY) license (https://creativecommons.org/licenses/by/4.0/).

1. Introduction

Heat transfer fluids (HTFs) play a key role in several application areas, from human bodies to engineering systems. Heat transfer processes are deeply important in heat exchangers and, consequently, the chemical and thermophysical characteristics of the working fluids can affect the overall heat to power efficiency. Therefore, enhancement of thermophysical properties like specific heat, thermal conductivity, stability, materials compatibility and viscosity have gained much attention from researchers in the past decade [1].

From nuclear reactors, where thermal energy is released by fission, up to thermodynamic power systems, HTFs are involved in different operating steps, and several studies were performed over the years to select the highest-performing thermal fluids [2]. HTF

selection is a crucial parameter also for renewable energy technologies such as thermal solar energy plants, as it strongly affects the economic effectiveness and dispatchability of these systems [3].

An ideal heat transfer fluid should possess favorable thermo-physical properties and should be chemically stable, non-corrosive, non-toxic, non-flammable and able to operate over a large temperature range without undergoing any adverse changes. Though water is the most obvious choice as a primary working fluid, it has limitations in terms of operating temperatures and pressures, hence the necessity to develop more suitable thermal exchange fluids that can efficiently operate at high temperatures. The modern HTFs are mainly synthetic, and, among them, thermal oils can operate, pressurized with an inert gas, at temperatures of up to 400 °C [4], whereas mineral and hot oils are generally thermally stable up to a maximum temperature of 300 °C [4]. For this reason, aromatic species such as Therminol 66 and Dowtherm Q are typically employed in nuclear and solar plants [5,6].

Unlike other oil-based materials [7,8], very little data are currently available about thermal oil's chemical stability and possible composition changes as a function of the operating temperatures. Actually, the instability near and above the maximum operating temperature represents one of the most critical limitations for these materials due to the occurrence of modifications in their chemical structure along with production of flammable gasses like, for instance, hydrogen. In addition, the degradation reactions could lead to a worsening of the fluids in thermo-physical features and to fouling processes, resulting in circuitry pollution [9–11]. Since the former and more traditional application of oils was as coolants in the nuclear field, these materials have been generally characterized and tested under simultaneous heat and irradiation stress [12,13], and only a small amount of material is available in the scientific literature regarding their thermal stability [14]. Silicone oils, unlike hydrocarbon analogs, are scarcely flammable and, hence, they are more popular for applications in which the fire safety and ecologic requirements are high, additionaaly, in recent years, they have gained great interest also as cooling media for Lithium-Ion Battery (LIB) modules [15] and, in general, for electronics systems [16]. These organosilicone fluids possess a unique combination of properties and are virtually chemically and corrosion inert, non-explosive and low in terms of toxicity. According to manufacturer recommendations [17–20] silicone oils are suitable for operation at temperatures of up to 400 °C in a closed-loop system and 250 °C in open systems. However, the low volatility and the characteristics of these compounds suggest that they can present greater thermal stability.

Currently, very few investigations have reported on their possible utilization as HTFs at medium-high temperature despite the fact that they might represent a very innovative alternative to other heat transfer media for CSP (Concentrating Solar Plants) applications, especially considering parabolic trough configurations, where the operating temperature ranges typically from around 200 °C up to 400–500 °C [5]. Actually, polymeric siloxanes are costly and present high viscosity values, but they can be considered as an alternative to the currently used aromatic oils, given a higher thermal resistance (shown in this work) and a lower volatility. A key point for the evaluation of these materials as proper HTFs is the investigation of their chemical stability over the requested working temperature; in this regard, Jung et al. [21] evaluated the employment of a commercial PDMS as an alternative to aromatic thermal oils in parabolic CSP, concluding that, thanks to a greater thermal resistance, its utilization can lead to a reduction in the plant's levelized costs of electricity (LCOE) of up to 5%. Other data are present regarding the degradation process of polysiloxanes species present in hydrocarbon mixtures [22,23]. Concerning the thermal behavior of single siloxanes, several studies were published about hexamethyldisiloxane (MM) and octamethyltrisiloxane (MDM) being used as working fluids for organic Rankine cycles (ORCs) [24–28].

As a possible alternative to PDMS, the purpose of this work is to study the thermal stability characteristics of a methyl phenyl silicone oil, Bluesil FLD 550 HT, considering its thermal degradation behavior under an inert gas of up to 450 °C. Moreover, it also investigated the effect of the thermal aging process on the fluid thermophysical features. The obtained results were compared to the ones of different aromatic oils, namely, a terphenyl-based thermal oil commercially known as Therminol 66 [29] and a mixture of C13-C20 substitute benzene, Therminol SP [30].

2. Materials and Methods

For this study a methyl phenyl siloxane co-polymer, commercially known as Bluesil FLD 550 HT [31] (Bluestar silicones, France), was selected as a representative of the silicone-based oils category. Its main thermos physical properties are summarized in Table 1.

Table 1. Thermophysical characteristics of Bluesil 550 HT [31].

Thermophysical Characteristics	
Composition	Methyl Phenyl siloxane co-polymer
Color	colorless
Viscosity at 25 °C, mm^2/s, approx	125
Specific gravity at 25 °C, approx	1.065
Flash point, °C, approx	300
Freezing point, °C	−50
Refractive index at 25 °C, approx	1.495
Surface tension at 25 °C, mN/m, approx	24.5
Vapor pressure at 200 °C, mbar, approx	1.33×10^{-2}
Expansion coefficient between 25 °C and 100 °C, approx	7.5×10^{-4}
Specific heat between 40 °C and 200 °C J/gK approx	1.50
Thermal conductivity, W/mK approx	0.15
Viscosity, mm^2/s, approx.:	
at 100 °C	20
at 35 °C	84
at 25 °C	125
at −30 °C	22,000

The experimental procedure was the same as described in previous works [29,30]; a batch lab-scale dedicated experimental set-up was designed and built for a better understanding of the thermal degradation processes involved in the aging of the oil. A schematic representation is reported in Figure 1.

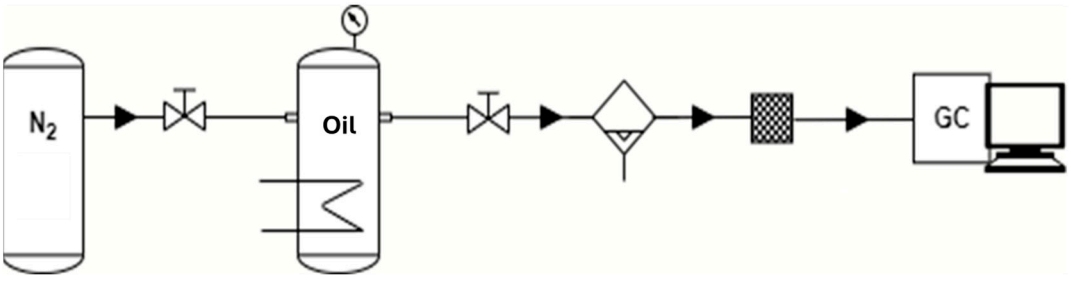

Figure 1. Schematic representation of the experimental set-up. In the picture, from the left: nitrogen tank, electrically heated reactor, condensation trap for the condensable products collection, silica trap and the Micro GC with flow controller.

The oil samples (300 mL) were inserted into a stainless-steel container (AISI 304) under a nitrogen atmosphere. The temperature was set and controlled by a PID system, and each oil sample was kept under isothermal conditions for a certain time (3 h); then, the main decomposition products were analyzed. The condensable products from the

vapor fraction were collected and analyzed with a gas chromatograph coupled with mass spectrometry instrument, described below. The permanent gas volume fractions were measured by a gas chromatograph. More thermally stressed oil samples (3 h at 475 °C) were taken as references of "aged material" to be compared with fresh (unheated) samples; a different analytical technique, described in the following sections, was used in this study. A kinetics degradation model was developed to describe the oil's behavior in the tested temperature range. To estimate the degradation kinetics rate, some assumptions were necessary; in particular, hydrogen was assumed to be the main product at the investigated temperatures, and its formation was used as an indicator of oil degradation, considering only qualitatively other possible reactions, such as methane production. The back reaction was neglected, given the products were continuously removed by the nitrogen flow. Also, the oil's initial number of moles are considered to be practically unchanged due to their negligible degradation percentage. Considering the batch configuration and a first-order reaction, the Arrhenius constant can be obtained as follows:

$$C_t = \frac{\left(C_0 * V_o - C_{H_2} * V_{hs}\right)}{V_o} \quad (1)$$

$$ln^{C_0}/_{C_t} = k * t \quad (2)$$

$$k = A * e^{-E_a/RT} \quad (3)$$

where

Co = initial terphenyl concentration [mol/L]
Vo = oil volume [L]
Ct = terphenyl concentration [mol/L]
Vhs = head space volume [L]
C_{H2} = Hydrogen concentration [mol/L]
K = Arrhenius constant
t = time [min]
T = temperature [K]
A = pre-exponential factor
Ea = activation energy [kJ/mol]
R = 8.314 [J/mol K]

Instrumentation

The evolution of the permanent gasses, hydrogen and methane, was monitored with a MicroGC 4900 Varian, equipped with a molecular sieve (MS5) column for hydrogen detection and a poraplot Q column for methane and volatile hydrocarbons; in both cases a TCD-type detector was used, with Argon functioning as a carrier gas. The precision of the obtained data was conservatively evaluated according to an estimation of the instrumental errors provided by the GC calibration curve for hydrogen.

Degradation products condensable at room temperature were analyzed by an Agilent Gas Chromatograph coupled with a mass spectrometer, and it has a capillary column (Alltech Capillary Column Phase: AT-WAX), with a length of 25 m, an external diameter of 0.53 mm and a film thickness of 1.2 μm. A NIST mass spectra library [32] was used to identify the compounds characterized by the most intense peaks. Each sample (100 ppm) was prepared in cyclohexane and analyzed under 0.7 mL/min of Helium as carrier gas, imposing as the temperature program a ramp of 10 °C/min up to 500 °C.

A thermogravimetric analysis was performed to evaluate the volatility of the oils as a function of temperature with an accuracy of ±1 °C. With this purpose, the TGA

output curves were analyzed considering the onset degradation temperature as the value at which the oil loses 3% of its initial weight. The measurements were carried out both under nitrogen and air atmosphere using a Mettler Toledo (Greifensee, Switzerland) (TGA/DSC 1) thermogravimetric analyzer. Around 20 µL of sample are placed in a 70 µL alumina crucible and positioned into the furnace.

Specific heat was measured with a Differential Scanning Calorimetry (Mettler Toledo DSC1), according to the DIN51007 methodology [33], using a Sapphire standard. Measurements were carried out from room temperature up to 240 °C (ramp of 10 °C/min) in 40 µL alumina crucibles under nitrogen (20 Nml/min).

Viscosity measurements up to 100 °C were performed with a rotational-type rheometer (TA AR2000 ex, TA Instruments, New Castle, DE, USA) with parallel plates. Viscosity was evaluated at four different temperatures, from 40 °C to 100 °C, over a programmed shear rate range (from 100 s^{-1} up to 1000 s^{-1} and vice versa).

Both for specific heat and viscosity measurements, ten different measurements were carried out for each sample to evaluate the precision of the results (Equations (4)–(6)).

$$X_m = \frac{\sum_{n=1}^{10} X_i}{N} \quad (4)$$

$$Err_m = \frac{2 * \sigma}{\sqrt{N}} \quad (5)$$

$$Err_{\%} = {}^{Err_m}/_{X_m} * 100 \quad (6)$$

where

X_m = average measured value [J/g*K]
X_i = measured values [J/g*K]
N = measurements number
σ = standard deviation
Err_m = mean error
$Err_{\%}$ = precision percentage error

Instrumental accuracy, for viscosity measurement, was calculated in accordance with Equation (7) [34] using a standard material known as N100 [35].

$$Err_{\%} = \frac{(|X_{Th} - X_m|)}{X_{Th}} * 100 \quad (7)$$

where

X_m = average measured value [Pa*s]
X_{Th} = value from technical data sheet [Pa*s]

An infrared analysis was used to track the thermal oil behavior by overlapping the spectra obtained from fresh (unheated) and aged (heated) oil samples using a Perkin Elmer spectrometer with an operative wavenumber range of 350–7800 cm^{-1}. The device is equipped with an ATR (attenuated total reflection) module with a zinc selenide (ZnSe) crystal.

3. Results

An amount of 300 mL of Bluesil 550 HT sample was tested at nominal temperatures of 425, 450 and 475 °C, with the results from the latter temperature acting as a reference for the mostly aged material. The GC experimental results obtained allow for the quantitative measuring of the permanent gasses produced during the reaction period, as shown in Table 2. The gaseous, non condensable stream contains quite a significant amount of

hydrogen together with methane. Additionally, ethane, ethylene and carbon dioxide were detected at all reaction temperatures, in good accordance with the behavior reported for the thermal decomposition of MM and MDM siloxanes [26,28], but in very small quantities, close to the instrument detection limit.

Table 2. Measured Hydrogen and Methane (μmol/grams of oil) as a function of temperature.

T_{set} (°C)	T_{oil} (°C)	H_2 (μmol/g)	CH_4 (μmol/g)
425	403	27	26
450	428	85	37
475	453	529	79

From the comparison of the hydrogen and methane production rates, reported in Figure 2, it is clearly visible that the dependence on temperature is much greater for hydrogen formation. The slope of the line in Figure 3 provides the activation energy of the degradation process (202.4 kJ/mol). A 10% experimental error, according to GC accuracy, was considered.

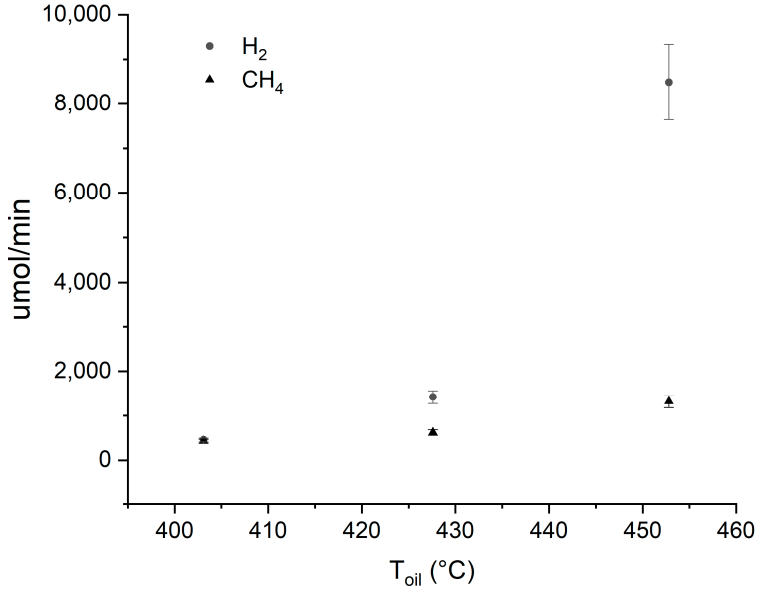

Figure 2. Hydrogen and methane production rate as a function of temperature. The bars across the symbols stand for the experimental errors calculated according to instrumental accuracy.

The hydrogen production rate at 425 °C is very similar to the one reported at the same temperature after 3000 s for the thermal decomposition of a PDMS [21].

Confronted with the chemical stability of other oils, hydrogen production by thermal degradation was previously investigated for Therminol 66 [29] and Therminol SP [30] with the same experimental equipment and by testing the same amount (300 mL) of oil, with activation energies of, respectively, 166.5 kJ/mol and 280.6 kJ/mol. In Table 3, the literature data are compared with the ones of Bluesil 550 HT. Although no methane was produced with the aromatic oils, it clearly resulted in greater stability for the silicone fluid, for which a gas partial pressure of 8 bar was reached at 475 °C, while 12 bar of gas was produced at 405 °C with Therminol SP. Also, the amount of produced condensable materials is far more relevant for the Therminol oils.

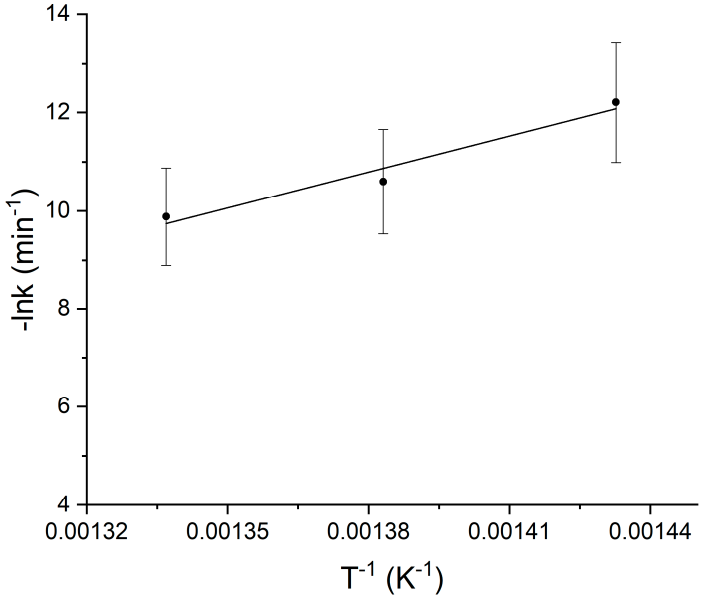

Figure 3. Plot to obtain the activation energy (Ea, curve slope) and pre-exponential factor (A, from the curve intercept on the ordinate) regarding the kinetics for hydrogen production. The bars across the symbols stand for the experimental errors calculated according to instrumental accuracy.

Table 3. Summary results of the thermal stability tests results, comparison with Therminol 66 [29] and Therminol SP [30].

Tested Oil	Temperature Range Tested	Overheating Temperature	Partial Pressure Reached	Amount of Condensable Production
	°C	°C	bar	mL
Therminol66 [29]	350–415	430	9	35
Therminol SP [30]	350–390	405	12	25
Bluesil	400–475	475	8	8

Figure 4 shows the GC-MS analysis performed on the condensable fraction produced by Bluesil 550 HT at the highest decomposition temperature (475 °C); the main compounds were identified by the NIST [32] and are reported. Bluesil behavior is similar to PDMS, with cyclic and linear siloxanes acting as main elements [22,23].

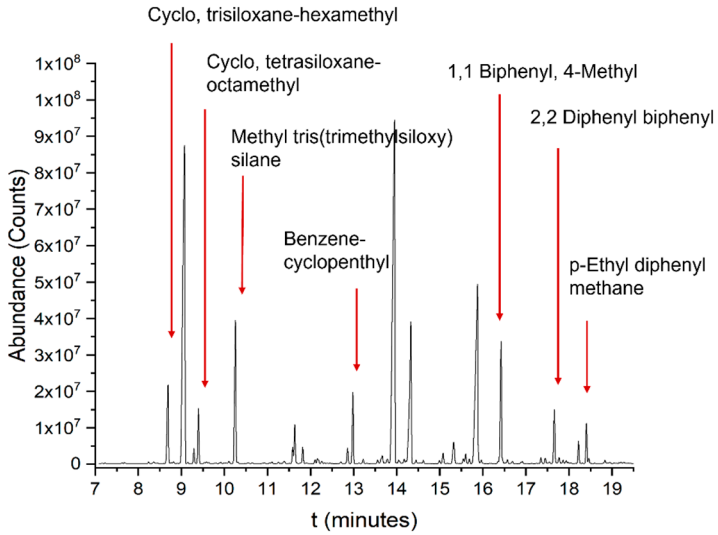

Figure 4. GC-MS analysis of the degradation products at 475 °C condensable at room temperature, with main compounds identified (NIST library).

4. Discussion

According to the literature data, polymeric siloxane compounds under thermal stress react through two main competitive degradation routes: a molecular mechanism which implies Si-O bond scission takes place with the formation of cyclic oligomers, and the rearrangement of the silicone–oxygen bonds leads to volatile byproducts. Also, a radical mechanism, which prevails at high temperatures, occurs by a homolytic Si-CH_3 bond scission and leads to methane (Figure 5) and hydrogen release, with the formation of cross-linked materials by oxidation with peroxyl compounds increasing fluid viscosity [36–38]. Therefore, methane and hydrogen production can be considered as processes occurring in series.

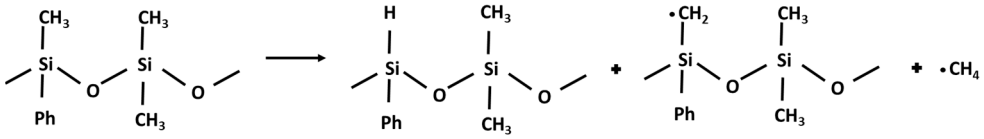

Figure 5. Reaction mechanism for methane production.

It is important to note that no solid byproducts were detectable in the aged oil, indicating the absence of fouling.

Thermogravimetric curves acquired on fresh and aged Bluesil samples are shown in Figure 6; initial decomposition temperatures are very high for fresh Bluesil, with values of 375.5 °C under nitrogen and 374 °C under air. A very interesting result was obtained for the aged Bluesil under nitrogen, where the onset temperature strongly decreased to 185 °C, probably due to siloxane chain fragmentation processes.

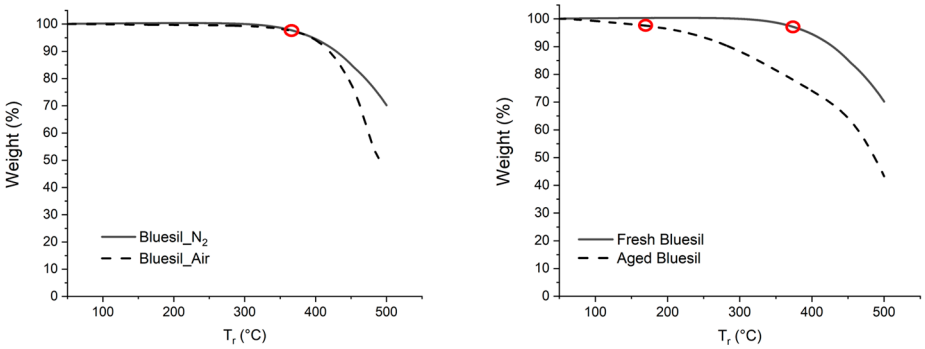

Figure 6. On the left: the TGA of fresh Bluesil both under 20 Nml of nitrogen (continuous curve) and air (dashed curve), onset temperatures are highlighted (red circles); the oxygen presence effects on the Bluesil volatility are limited. On the right: Fresh (continuous curve) and aged (dashed curve) Bluesil thermogravimetric curves under nitrogen, onset temperatures are highlighted (red circles); the volatility decreases significantly in the aged sample.

In previous work [29,30], the same analysis was performed for Therminol 66 and Therminol SP. The onset temperatures are summarized in Table 4. Although fresh Therminol 66 seems to be less stable than fresh Therminol SP, the volatility of the latter undergoes to a strong decrease with the thermal aging processes, and this explains the pressure values reached during the heating process. Fresh Bluesil, as expected, given the higher dissociation energy of Si-O bond compared to C-C bond [39] ($\Delta Hf_{Si\text{-}O}$ = 798 kJ/mol, $\Delta Hf_{C\text{-}C}$ = 607 kJ/mol), has a much higher stability with respect to aromatic oils [21]; however, a strong volatility increase was observed in the aged sample. Finally, thermal stability was slightly changed in the thermally stressed Therminol 66.

Table 4. Onset temperatures of fresh and aged oils obtained from TGA.

Tested Oil	Fresh Oil Onset Temperature (°C)	Aged Oil Onset Temperature (°C)
Therminol 66 [29]	215	223
Therminol SP [30]	244	177
Bluesil	376	185

Specific heat measurements, along with a confrontation regarding the literature data, are reported in Figure 7, with a resulting relative error of below 5%. It can be concluded that, considering the experimental error, specific heat does not change significantly during the aging process.

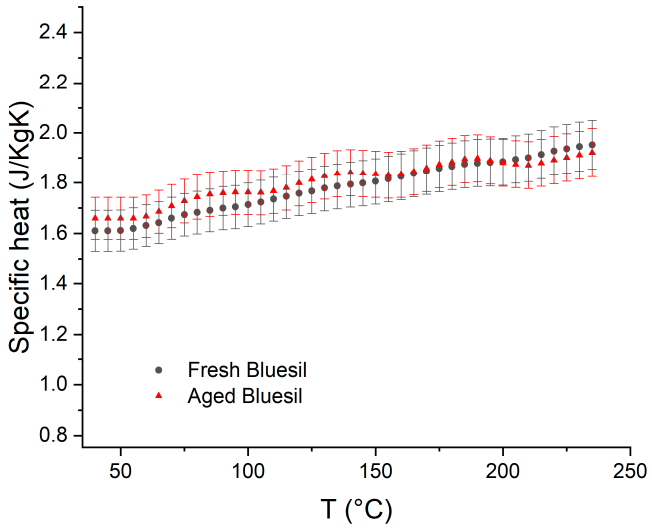

Figure 7. Comparison between fresh (black) and aged (red) Bluesil specific heat. No significant changes were detected within the experimental error.

Calorimetric measurements for fresh and aged Therminol 66 and Therminol SP [29,30] are summarized in Table 5. In addition to their specific heat values, their dependance in regard to temperature does not significantly change in the temperature range, with Bluesil presenting the smaller specific heat values and the lower dependence on temperature.

Table 5. Fitting equations based on calorimetric measurements on fresh and aged Therminol 66 and Therminol SP.

Thermally Stressed Oils	Fresh Oil Onset Fitting Equations	Aged Oil Onset Fitting Equations
Therminol 66 [29]	$Cp\ [KJ/Kg\ K] = 1.55 + 3.34 \times 10^{-3}\ T\ [°C]$	$Cp\ [KJ/Kg\ K] = 1.54 + 3.21 \times 10^{-3}\ T\ [°C]$
Therminol SP [30]	$Cp\ [KJ/Kg\ K] = 1.91 + 3.04 \times 10^{-3}\ T\ [°C]$	$Cp\ [KJ/Kg\ K] = 1.96 + 3.47 \times 10^{-3}\ T\ [°C]$
Bluesil	$Cp\ [KJ/Kg\ K] = 1.53 + 1.81 \times 10^{-3}\ T\ [°C]$	$Cp\ [KJ/Kg\ K] = 1.62 + 1.36 \times 10^{-3}\ T\ [°C]$

Table 6 and Figure 8 show the viscosity values for the fresh and thermally stressed Bluesil samples.

Dynamic viscosity increases for the thermal stressed sample; although the effect is limited, it is still detectable considering 10% of the measured experimental error, especially at lower temperatures. The reason for this was explained above, and it is due to the formation of cross-linked high-viscous polymers [36].

Fresh Therminol 66 [29] and Therminol SP [30] show similar viscosity values (Figure 9) in the tested temperature range but an opposite trend with respect to thermal aging; a

strong increase was observed for Therminol 66, while Therminol SP underwent a viscosity decrease. Both the obtained results agree with the TGA degradation onset temperatures; viscosity increasing together with the volatility drop indicate that Therminol 66 thermal aging occur mainly through polymerization processes, while thermal cracking prevails for Therminol SP.

Table 6. Rheometric comparison between fresh and aged Therminol 66 with percentage differences.

T	Fresh_Bluesil	Aged_Bluesil	Diff
°C	Pa*s	Pa*s	%
40	6.85×10^{-2}	8.56×10^{-2}	20.0
60	3.81×10^{-2}	4.33×10^{-2}	11.9
80	2.43×10^{-2}	2.54×10^{-2}	4.30
100	1.77×10^{-2}	1.59×10^{-2}	11.2

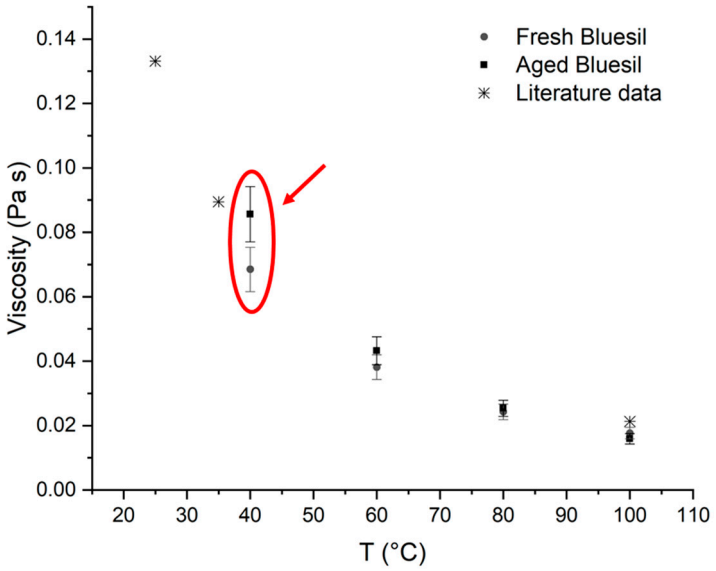

Figure 8. Comparison between the viscosities of fresh and aged Bluesil; the literature data are also reported. A detectable viscosity increase in aged Bluesil can be observed, and differences between fresh and aged samples are particularly marked at lower temperatures (red circle).

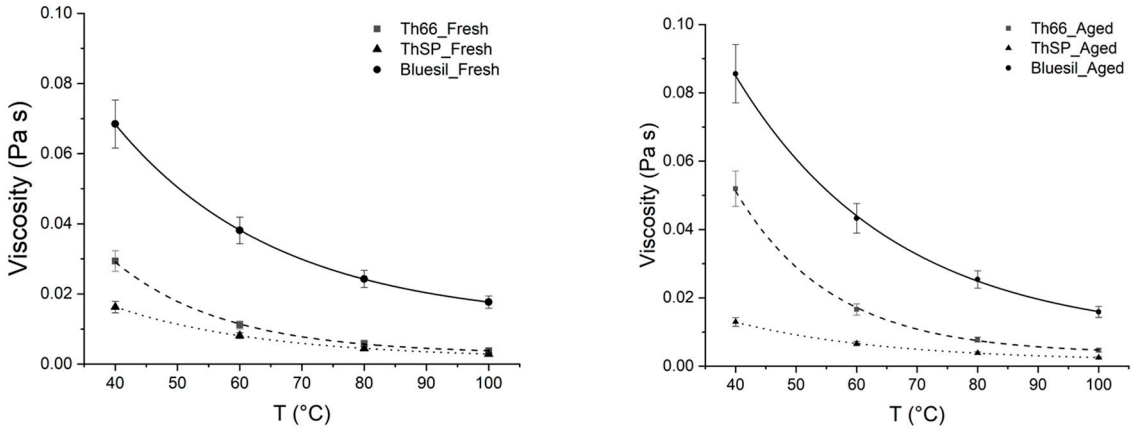

Figure 9. Comparison of viscosity measurements performed on fresh (**left**) and aged (**right**) oil samples. Error bars, according to experimental error, are also reported.

Bluesil viscosity is much higher with respect to the other oils both in fresh and aged samples; the above citated molecular mechanisms explain the TGA and rheometric results.

Regarding the IR analysis of fresh and aged Bluesil, the infrared spectra are reported together in Figure 10, showing a small increase in the Si-O-Si peak intensity, which can be realistically associated with the formation of cross-linked bonds during the degradation bond, as discussed above; this result is congruent with the increase in dynamic viscosity for thermally stressed samples. Additionally, the overall chemical structure can be considered to be only slightly affected due to the minor extent of chemical degradation.

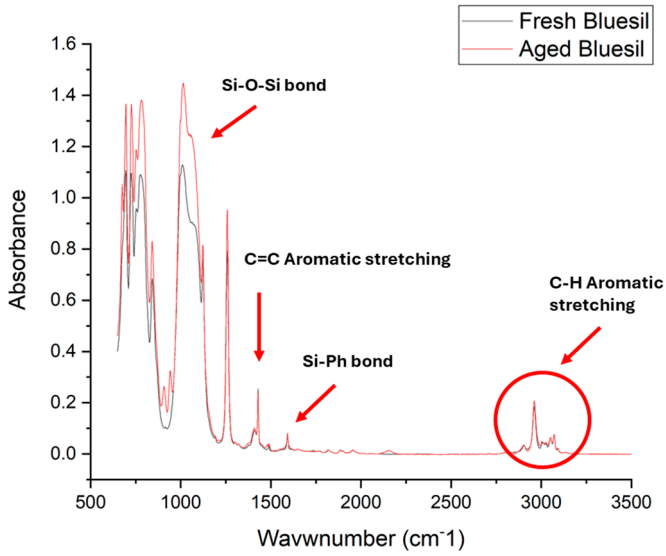

Figure 10. Infrared spectra analysis of fresh and aged Bluesil. The black line stands for the fresh sample and the red line stands for the aged sample.

5. Conclusions

The results obtained in this work confirmed the Bluesil low volatility and good chemical stability up to 450 °C under a nitrogen atmosphere. This behavior is comparable to the one reported for DPMS studied under similar conditions. Hydrogen is the main degradation product, and it is possible to assume a partial segmentation of the silicone chains, indicated by an increase in the fluid viscosity, due to the formation of cross-linked compounds. However, the extent of these variations is limited, even at 450 °C, as demonstrated by calorimetric, chromatographic and spectroscopic analyses, which show that only small changes are produced regarding specific heat and oil composition. A kinetic equation was defined regarding the hydrogen production rate, which can be used to estimate a realistic lifetime for the fluid at different temperatures.

A comparison with commercial thermal oils shows the expected higher chemical resilience of the siloxanes structure with respect to the aromatic one, resulting in an increase in the maximum temperature limit of about 100 °C for Bluesil. This feature can make silicone oils quite interesting for CSP applications, considering their low flammability. On the other hand, their high price still represents a disadvantage for large utilization in solar power plants.

Therminol 66 and Therminol SP present different degradation processes, that is, polymerization for the former and molecular cracking for the latter.

Author Contributions: Conceptualization, E.M., G.T. and S.S.; Methodology, E.M., I.B., G.T., A.C.T. and A.C.; Software, I.B., G.C., F.F., N.R. and A.S. (Andrea Simonetti); Validation, S.S.; Formal analysis, N.C., N.R., A.S. (Annarita Spadoni) and A.C.T.; Investigation, E.M., G.C., F.P. and A.S. (Andrea Simonetti); Data curation, E.M., N.C., F.P., S.S., A.S. (Annarita Spadoni) and A.C.T.; Writing—original draft, E.M.; Writing—review & editing, I.D.S., S.S., A.C.T. and A.C.; Visualization, I.D.S. and F.F.;

Supervision, A.C. and M.C.; Project administration, A.C. and M.C.; Funding acquisition, M.C. All authors have read and agreed to the published version of the manuscript.

Funding: This research was funded by French Alternative Energies and Atomic Energy Commission.

Data Availability Statement: The original contributions presented in this study are included in the article. Further inquiries can be directed to the corresponding author.

Acknowledgments: This work was developed in the framework of the ARDECO project (ASTRID Research and Development Cooperation) CEA-ENEA agreement; the authors are grateful for the revision and suggestions provided by their CEA colleagues. The presented work is also part of a doctoral thesis coordinated by M.C. Annesini, whom the authors would like to thank.

Conflicts of Interest: The authors declare no conflict of interest.

Abbreviations

The following abbreviations are used in this manuscript:

HTF	Heat transfer fluid
HT	Heat transfer
GC	Gas chromatograph
TCD	Thermal conductivity detector
GC-MS	Gas chromatography coupled to mass spectrometry
TGA	Thermo gravimetric analysis
DSC	Differential scanning calorimetry

References

1. Krishna, Y.; Faizal, M.; Saidur, R.; Ng, K.; Aslfattahi, N. State-of-the-Art Heat Transfer Fluids for Parabolic Trough Collector. *Int. J. Heat Mass Transf.* **2020**, *152*, 119541. [CrossRef]
2. El-Genk, M.S.; Tournier, J.-M. On the Use of Noble Gases and Binary Mixtures as Reactor Coolants and CBC Working Fluids. *Energy Convers. Manag.* **2008**, *49*, 1882–1891. [CrossRef]
3. Lorenzin, N.; Abánades, A. A Review on the Application of Liquid Metals as Heat Transfer Fluid in Concentrated Solar Power Technologies. *Int. J. Hydrogen Energy* **2016**, *41*, 6990–6995. [CrossRef]
4. Benoit, H.; Spreafico, L.; Gauthier, D.; Flamant, G. Review of Heat Transfer Fluids in Tube-Receivers Used in Concentrating Solar Thermal Systems: Properties and Heat Transfer Coefficients. *Renew. Sustain. Energy Rev.* **2016**, *55*, 298–315. [CrossRef]
5. Giaconia, A.; Tizzoni, A.C.; Sau, S.; Corsaro, N.; Mansi, E.; Spadoni, A.; Delise, T. Assessment and Perspectives of Heat Transfer Fluids for CSP Applications. *Energies* **2021**, *14*, 7486. [CrossRef]
6. Vutukuru, R.; Pegallapati, A.S.; Maddali, R. Suitability of Various Heat Transfer Fluids for High Temperature Solar Thermal Systems. *Appl. Therm. Eng.* **2019**, *159*, 113973. [CrossRef]
7. Campuzano, F.; Ordoñez, J.; Martínez, J.D.; Agudelo, A.F.; Sarathy, S.M.; Roberts, W.L. Thermal Decomposition Characteristics of the Tire Pyrolysis Oil Derived from a Twin-Auger Reactor: Study of kinetics and Evolved Gases. *Fuel* **2023**, *338*, 127248. [CrossRef]
8. Santos, J.C.O.; dos Santos, I.M.G.; Souza, A.G.; Sobrinho, E.V.; Fernandes, V.J., Jr.; Silva, A.J.N. Thermoanalytical and Rheological Characterization of Automotive Mineral Lubricants after Thermal Degradation. *Fuel* **2004**, *83*, 2393–2399. [CrossRef]
9. Ikonen, E.; Liukkonen, M.; Hansen, A.H.; Edelborg, M.; Kjos, O.; Selek, I.; Kettunen, A. Fouling Monitoring in a Circulating Fluidized Bed Boiler Using Direct and Indirect Model-Based Analytics. *Fuel* **2023**, *346*, 128341. [CrossRef]
10. Yang, Q.; Tong, S.; Tong, Z.; Wang, H.; Cao, X.E. Ash Fouling Characteristic Analysis and Prediction for Pillow Plate Heat Exchanger in Waste Heat Recovery Based on Attentive-Feature Decision Algorithm. *Fuel* **2024**, *372*, 132133. [CrossRef]
11. Wang, F.-L.; Tang, S.-Z.; He, Y.-L.; Kulacki, F.A.; Yu, Y. Heat Transfer and Fouling Performance of Finned Tube Heat Exchangers: Experimentation via on Line Monitoring. *Fuel* **2019**, *236*, 949–959. [CrossRef]
12. Cellini, R.F. JEN Research Programme on Organic Moderator-Coolants. In Proceedings of the Panel on the Use of Organic Liquids as Reactor Coolants and Moderators, Vienna, Austria, 9–13 May 1966; pp. 67–93. Available online: http://www.iaea.org/inis/collection/NCLCollectionStore/_Public/34/065/34065185.pdf (accessed on 25 January 2025).
13. Smee, J.L.; Puttagunta, V.R.; Robertson, R.F.S.; Hatcher, R. *Organic Coolant Summary Report (No. AECL–4922)*; Atomic Energy of Canada Ltd.: Chalk River, ON, Canada, 1975.

14. Grirate, H.; Zari, N.; Elmchaouri, A.; Molina, S.; Couturier, R. Life Time Analysis of Thermal Oil Used as Heat Transfer Fluid in CSP Power Plant. In Proceedings of the SOLARPACES 2015: International Conference on Concentrating Solar Power and Chemical Energy Systems, Cape Town, South Africa, 13–16 October 2015. [CrossRef]
15. Cheng, W.; Chen, M.; Ouyang, D.; Weng, J.; Zhao, L.; Chen, Y. Investigation of the Thermal Performance and Heat Transfer Characteristics of the Lithium-Ion Battery Module Based on an Oil-Immersed Cooling Structure. *J. Energy Storage* **2024**, *79*, 110184. [CrossRef]
16. Lin, Y.-H.; Kang, S.-W.; Wu, T.-Y. Fabrication of Polydimethylsiloxane (PDMS) Pulsating Heat Pipe. *Appl. Therm. Eng.* **2009**, *29*, 573–580. [CrossRef]
17. Silicones, Organo Functional. 2011. 'BLUESIL'. Available online: https://www.bag-distribution.com/Files/108113/16311264463191.pdf (accessed on 12 January 2025).
18. Dow. n.d. SYLTHERMTM XLT Heat Transfer Fluid Technical Data Sheet. Available online: http://www.dowtherm.com (accessed on 12 January 2025).
19. Thermal Expansion of SYLTHERM HF Fluid. n.d. Available online: www.dowtherm.com (accessed on 12 January 2025).
20. Typical Properties of SYLTHERM 800 Fluid 1. n.d. Available online: www.dowtherm.com (accessed on 12 January 2025).
21. Jung, C.; Dersch, J.; Nietsch, A.; Senholdt, M. Technological Perspectives of Silicone Heat Transfer Fluids for Concentrated Solar Power. *Energy Procedia* **2015**, *69*, 663–671. [CrossRef]
22. Chainet, F.; Le Meur, L.; Lienemann, C.-P.; Ponthus, J.; Courtiade, M.; Donard, O.F.X. Characterization of Silicon Species Issued from PDMS Degradation Under Thermal Cracking of Hydrocarbons: Part 1—Gas Samples Analysis by Gas Chromatography-time of Flight Mass Spectrometry. *Fuel* **2013**, *111*, 519–527. [CrossRef]
23. Chainet, F.; Le Meur, L.; Lienemann, C.-P.; Ponthus, J.; Courtiade, M.; Donard, O.F.X. Characterization of Silicon Species Issued from PDMS Degradation Under Thermal Cracking of Hydrocarbons: Part 2—Liquid Samples Analysis by a Multi-Technical Approach Based on Gas Chromatography and Mass Spectrometry. *Fuel* **2014**, *116*, 478–489. [CrossRef]
24. Dai, X.; Shi, L.; Qian, W. Thermal Stability of hexamethyldisiloxane (MM) as a Working Fluid for Organic Rankine Cycle. *Int. J. Energy Res.* **2019**, *43*, 896–904. [CrossRef]
25. Gallarini, S.; Spinelli, A.; Lietti, L.; Guardone, A. Thermal Stability of Linear Siloxanes and Their Mixtures. *Energy* **2023**, *278*, 127687. [CrossRef]
26. Keulen, L.; Gallarini, S.; Landolina, C.; Spinelli, A.; Iora, P.; Invernizzi, C.; Lietti, L.; Guardone, A. Thermal Stability of Hexamethyldisiloxane and Octamethyltrisiloxane. *Energy* **2018**, *165*, 868–876. [CrossRef]
27. Di Marcoberardino, G.; Invernizzi, C.M.; Iora, P.; Arosio, L.; Canavese, M.; Lunghi, A.; Mazzei, A. Thermal Stability and Thermodynamic Performances of Pure Siloxanes and Their Mixtures in Organic Rankine Cycles. *Energies* **2022**, *15*, 3498. [CrossRef]
28. Wang, W.; Dai, X.; Shi, L. Influence of Thermal Stability on Organic Rankine Cycle Systems Using Siloxanes as Working Fluids. *Appl. Therm. Eng.* **2022**, *200*, 117639. [CrossRef]
29. Mansi, E.; Sau, S.; Balog, I.; Caputo, G.; Corsaro, N.; Tiranti, G.; Filippi, F.; Panza, F.; Ratto, N.; Simonetti, A.; et al. High Temperature Stability of a Commercial Terphenyl-Based Thermal Oil. *Prog. Nucl. Energy* **2021**, *140*, 103900. [CrossRef]
30. Mansi, E.; Sau, S.; Balog, I.; Cemmi, A.; Ciotti, M.; Corsaro, N.; Caputo, G.; Filippi, F.; Panza, F.; Ratto, N.; et al. Oil Testing for Intense Use in CSP Applications. In Proceedings of the SOLARPACES 2020: 26th International Conference on Concentrating Solar Power and Chemical Energy Systems, Freiburg, Germany, 28 September–2 October 2020.
31. Bluesil Safety Data Sheet. 2016, pp. 1–16. Available online: https://www.siliconiitalia.it/public/schede/318/bluesil%20fld%20604v50%20in.pdf (accessed on 12 January 2025).
32. NIST. NIST Mass Spectral Database for NIST/EPA/NIH and Mass Spectral Search Program (Version 2.3). The National Institute of Standards and Technology NIST. Nist 17; 2017; pp. 1–73. Available online: http://www.nist.gov/srd/ (accessed on 8 January 2025).
33. Mettler. Thermal Analysis Specific Heat. 2003. Available online: http://www.mt.com/ta (accessed on 8 January 2025).
34. Taylor, J.R. *Introduction to Error Analysis: The Study of Uncertain*; University Science Books: Sausalito, CA, USA, 1997.
35. Cannon Instrument Company®. Viscosity & Flash Point Standards for Reference, Validation, and Calibration. n.d. Available online: www.cannoninstrument.com (accessed on 8 January 2025).
36. Zhou, W.; Yang, H.; Guo, X.; Lu, J. Thermal Degradation Behaviors of Some Branched and Linear Polysiloxanes. *Polym. Degrad. Stab.* **2006**, *91*, 1471–1475. [CrossRef]
37. Camino, G.; Lomakin, S.; Lageard, M. Thermal Polydimethylsiloxane Degradation. Part 2. The Degradation Mechanisms. *Polymer* **2002**, *43*, 2011–2015. [CrossRef]

38. Arkles, B. Silicone Fluids: Stable Inert Media. 1–30 January 2013. 2012. Available online: https://www.researchgate.net/publication/277313694_Silicone_Fluids_Stable_Inert_Media (accessed on 11 January 2025).
39. Bond Dissociation Energies Table. Available online: https://labs.chem.ucsb.edu/zakarian/armen/11---bonddissociationenergy.pdf (accessed on 11 January 2025).

Disclaimer/Publisher's Note: The statements, opinions and data contained in all publications are solely those of the individual author(s) and contributor(s) and not of MDPI and/or the editor(s). MDPI and/or the editor(s) disclaim responsibility for any injury to people or property resulting from any ideas, methods, instructions or products referred to in the content.